Palaeogeography, Palaeoclimatology, Palaeoecology 373 (2013) 88–97

Contents lists available at SciVerse ScienceDirect

Palaeogeography, Palaeoclimatology, Palaeoecology

journal homepage: www.elsevier.com/locate/palaeo

Preliminary evaluation of potential stable isotope and trace element productivity proxies in the oyster *Crassostrea gigas*

David H. Goodwin [a,*], David P. Gillikin [b], Peter D. Roopnarine [c]

[a] Department of Geosciences, Denison University, 100 West College Street, Granville, OH 43023, USA
[b] Department of Geology, Union College, 807 Union Street, Schenectady, NY 12308, USA
[c] Department of Invertebrate Zoology & Geology, California Academy of Sciences, 55 Music Concourse Drive, Golden Gate Park, San Francisco CA 94118, USA

ARTICLE INFO

Article history:
Received 30 June 2011
Received in revised form 15 March 2012
Accepted 26 March 2012
Available online 4 April 2012

Keywords:
Carbon isotope
Ba/Ca ratio
Phytoplankton bloom
Crassostrea gigas
San Francisco Bay
Paleoproductivity proxy

ABSTRACT

As most bivalve mollusks are filter feeders or deposit feeders—predatory septibranchs (Poromyacea) being the notable exception—they are closely linked with the activity of primary producers. Perhaps this is nowhere more evident than in shallow water habitats influenced by seasonal phytoplankton blooms. In these systems, photoautotrophs are capable of changing the physical and chemical properties of the water column. In turn, clams, ingest large quantities of phytoplankton and precipitate their shells in these chemically altered waters. Thus, clam shells likely archive valuable information about phytoplankton dynamics in shallow water habitats. To better understand this relationship, we investigated geochemical records from two potential productivity proxy systems archived in shells of the oyster *Crassostrea gigas* that live in the San Francisco Bay estuary, California, USA. Here we present multi-year records of shell carbon isotope ($\delta^{13}C_{carb}$) and barium/calcium (Ba/Ca_{carb}) variation. These archives are compared with records of environmental variation using oxygen isotopes ($\delta^{18}O_{carb}$) as a temporal marker. We also present high-resolution $\delta^{13}C_{carb}$, $\delta^{18}O_{carb}$ and Ba/Ca profiles associated with the 2003 spring phytoplankton bloom. Our results suggest that the prominent positive $\delta^{13}C_{carb}$ excursion, present in shell material deposited in the spring of 2003, most likely reflects photosynthetic enrichment of the dissolved inorganic carbon pool. Calibration of stable isotopes with calculated chlorophyll *a* concentrations, measured during the bloom, suggests that our $\delta^{13}C_{carb}$ sample variation reflects phytoplankton abundance with 3 to 4 day resolution. These findings highlight the potential utility of stable isotope records as tools for reconstructing patterns of primary productivity. Elevated Ba/Ca values are recorded each year in the spring. Thus, like stable isotope profiles, Ba/Ca profiles from these specimens demarcate individual years of shell growth and establish ontogenetic age. Low- and high-resolution Ba/Ca profiles do not, however, correlate with the 2003 spring phytoplankton bloom, casting doubt on the relationship between Ba/Ca ratios and phytoplankton blooms. Although the Ba/Ca peak timing loosely correlates with freshwater discharge events, peak amplitude does not, leaving the environmental cause/trigger of these peaks unknown. Nevertheless, the San Francisco Bay estuary seems like an ideal environment in which to further investigate the relationship between skeletal geochemical variation and patterns of primary productivity.

1. Introduction

In recent decades analysis of geochemical records from biogenic carbonates has become a nearly ubiquitous component of paleoenvironmental research. For example, seminal papers by Urey (1947), Urey et al. (1951) and Epstein et al. (1953) showed that oxygen isotope ratios in biogenic carbonates ($\delta^{18}O_{carb}$) are a function of temperature and the isotopic composition of water ($\delta^{18}O_{water}$). Later work on stable carbon isotopes in mollusk shells ($\delta^{13}C_{carb}$) by Mook and Vogel (1968), Fritz and Poplawski (1974) and Killingley and Berger (1979) highlighted their utility as recorders of dissolved inorganic carbon (DIC) variation. Tanaka et al. (1986), McConnaughey et al. (1997), Lorrain et al. (2004) and Gillikin et al. (2006a), however, showed that, like oxygen isotopes, carbon isotopes in shells reflect multiple environmental factors (i.e., dissolved inorganic carbon (DIC) and metabolic CO_2; see review by McConnaughey and Gillikin, 2008).

In addition to stable isotopes, elemental ratios have become an important tool for environmental reconstruction. Early studies of the elemental composition of invertebrate skeletons highlighted their potential as recorders of an animal's environment (e.g., Pilkey and Goodell, 1963; also see Vinogradov, 1953 for an early review). More recently, skeletal bound element ratios have been used in concert with stable isotopes to reconstruct past environmental conditions (e.g., Gillikin et al., 2006b and Gillikin et al., 2008).

One field of inquiry that stands to benefit from the marriage of stable isotope and elemental ratio analysis is paleoproductivity proxy

* Corresponding author.
E-mail addresses: goodwind@denison.edu (D.H. Goodwin), gillikid@union.edu (D.P. Gillikin), proopnarine@calacademy.org (P.D. Roopnarine).

0031-0182/$ – see front matter © 2012 Elsevier B.V. All rights reserved.
doi:10.1016/j.palaeo.2012.03.034

development. Many authors have observed that barium/calcium (Ba/Ca) profiles are characterized by relatively constant background values punctuated by distinct periodic peaks (Stecher et al., 1996; Vander Putten et al., 2000; Lazareth et al., 2003; Gillikin et al., 2006b). Furthermore, numerous studies have shown that Ba/Ca profiles are reproducible between specimens indicating at least partial environmental control of barium incorporation in shells (Vander Putten et al., 2000; Carré et al., 2006; Gillikin et al., 2008; Thébault et al., 2009). Vander Putten et al. (2000) and Lazareth et al. (2003) have suggested that Ba/Ca ratios in shells are related to phytoplankton blooms. Stecher et al. (1996) postulated that prominent Ba/Ca peaks may reflect barite ($BaSO_4$) formation associated with decaying phytoplankton immediately following blooms. Despite their promise, Vander Putten et al. (2000) and Gillikin et al. (2008) noted that peak magnitude was not correlated with chlorophyll *a* concentration ([chl *a*]).

Like Ba/Ca ratios, $\delta^{13}C_{carb}$ variation has been linked with primary productivity. Several recent studies (e.g., Lorrain et al., 2004; Gillikin et al., 2005, 2006a; Poulain et al., 2010) showed that approximately 10% of the carbon incorporated into shell carbonate is derived from internal respiration of particulate organic matter (POM) with very negative $\delta^{13}C$ values (marine phytoplankton $\delta^{13}C_{POC}$: −20 to −30, Mook and Tan, 1991). The remainder is derived from external inorganic sources (sea water $\delta^{13}C_{DIC}$: 0 to −2, Mook and Tan, 1991). Furthermore, the fraction of metabolically derived CO_2 increases through ontogeny (Lorrain et al., 2004; Gillikin et al., 2007). Chauvaud et al. (2011) expanded on this idea by detrending intra-annual $\delta^{13}C_{carb}$ profiles from juvenile scallops collected in Europe, thus removing this ontogenetic trend. They found that the lowest $\delta^{13}C_{carb}$ values are from shell material deposited in the late spring to early summer and speculated that this was due to abundant ^{12}C-enriched POM (i.e., phytoplankton). In contrast, Goodwin et al. (2010) documented a pronounced positive $\delta^{13}C_{carb}$ excursion in shell material deposited in the spring from multiple oysters living in San Francisco Bay, USA. They speculated that this ^{13}C-enrichment event reflected photosynthetic leveraging of the DIC pool by the 2003 spring phytoplankton bloom, which resulted in water with high $\delta^{13}C_{DIC}$ values.

To investigate these ideas, we present geochemical records from two potential productivity proxy systems ($\delta^{13}C_{carb}$ and Ba/Ca ratios) archived in shells of the oyster *Crassostrea gigas*. Recent work has shown that oyster shells provide reliable records of environmental variation (e.g., Kirby, 2000; Surge et al., 2001; Wisshak et al., 2009; Goodwin et al., 2010; Titschack et al., 2010; Harzhauser et al., 2011). The specimens used in this study grew in the San Francisco Bay estuary, a system characterized by pronounced seasonal phytoplankton blooms (Cloern, 1996). Inter-annual Ba/Ca profiles, representing the lifespan of the oysters, are related to previously published $\delta^{18}O_{carb}$ and $\delta^{13}C_{carb}$ records from the same specimens (Goodwin et al., 2010). These records are compared with patterns of inter- and intra-annual salinity, freshwater input, and [chl *a*] variation. In addition, new stable isotope and Ba/Ca profiles, which correspond to the well-documented 2003 spring phytoplankton bloom in south San Francisco Bay (see Luengen et al., 2007), are compared with daily temperatures and salinities as well as sub-weekly records of [chl *a*]. The goals of our study are threefold: 1) to document patterns of inter-annual variation of potential productivity proxies; 2) to calibrate geochemical variation with environmental records in a system with pronounced seasonal phytoplankton blooms; and, 3) to evaluate the synchrony of isotopic and trace element variation associated with high-resolution environmental variation during a large phytoplankton bloom.

2. Materials and methods

The study area is located in the San Francisco Bay (SFB) estuary on the north central coast of California, USA (see Goodwin et al., 2010: Fig. 1 for locality map). Marine water enters the estuary at the Golden Gate, while most of the freshwater input (~90%) is from flow of the Sacramento and San Joaquin rivers by way of the inland delta region (herein the Delta) (Conomos, 1979). The remainder comes from small local streams and municipal wastewater (Conomos, 1979). Freshwater input is highly seasonal, with the majority arriving in winter and early spring associated with storms and snowmelt (Conomos et al., 1979).

2.1. Environmental data

Environmental records were retrieved from several sources. Average daily water temperatures and salinities for the water years 2002–2006 (water year 5 October 1 through September 30) were calculated from measurements collected by U.S. Geological Survey near the east end of the Dumbarton Bridge. Measurements were taken 1 m below the surface every 15 min at the end of a fishing pier adjacent to the Bridge ~0.75 km from shore (37° 30.49′ N, 122° 07′ W; http://pubs.usgs.gov/wri/wri034005/). These data provide a nearly continuous record for the period, with occasional interruptions, most notably in 2005. Average daily Delta outflow entering San Francisco Bay was retrieved from the California Department of Water Resources Interagency Ecological Program for the 2002 through 2006 water years (http://iep.water.ca.gov/dayflow/). Chlorophyll *a* concentrations, calculated from fluorometer voltages calibrated with discrete measurements of [chl *a*], were collected by the U.S. Geological Survey at two locations in the South Bay (Station 30: 37° 33.3′ N, 122° 11.4′ W and Station 33: 37° 30.5′ N, 122° 7.3′ W; http://sfbay.wr.usgs.gov/access/wqdata). The average difference between paired discrete and calculated [chl *a*] samples collected between 2002 and 2006 was 1.1 μg/l (mean error 9.1%).

2.2. Specimens

The specimens used in this study were the subject of previous work by a subset of the authors (see Goodwin et al., 2010, for a detailed discussion). Specimens were collected alive from two localities on the eastern shore of south SFB (Hayward Landing: 37° 37.7′ N, 122° 9.1′ W; and, Dumbarton Bridge: 37° 30.6′ N, 122° 6.7′ W). Using $\delta^{18}O$ and $\delta^{13}C$ profiles, together with high-resolution records of environmental variability, Goodwin et al. (2010) identified two adult cohorts of the non-native oyster *Crassostrea gigas*. Based on the calibration of observed $\delta^{18}O_{carb}$ values (measured from sampled oyster shells) and predicted $\delta^{18}O_{carb}$ values (calculated from water temperatures and $\delta^{18}O_{water}$ values derived from salinity measurements), they determined that the first cohort arrived between 1998 and 2000 and the second in late 2001 or early 2002. The $\delta^{13}C$ profile from shells in the younger group (cohort 2) displays pronounced annual variation (see below). This cyclicity, however, is interrupted in 2003 by a distinctive positive anomaly, or "carbon spike." This study focuses on two specimens from cohort 2 (OY-018 from Hayward Landing and, OY-003 from farther south at Dumbarton Bridge).

2.3. Stable isotopes

Point samples (mass: ~50–100 μg) were hand-drilled from the foliated calcite layer by drilling down between 500 and 1000 μm into the ligamental area with a 300 μm diameter drill bit. In each specimen, samples were collected every ~500 to 1000 μm from the umbo to the ventral margin of the resilifer. The isotope profiles derived from these samples thus reflect environmental conditions experienced during the span of shell growth, from settlement to death (2002–2006). Additional details can be found in Goodwin et al. (2010). Throughout this manuscript, these profiles will be referred to as the "low-resolution" stable isotope profiles.

In addition, samples were micromilled from each specimen according to the procedures described by Dettman and Lohmann (1995). These samples were collected from a plane cut perpendicular

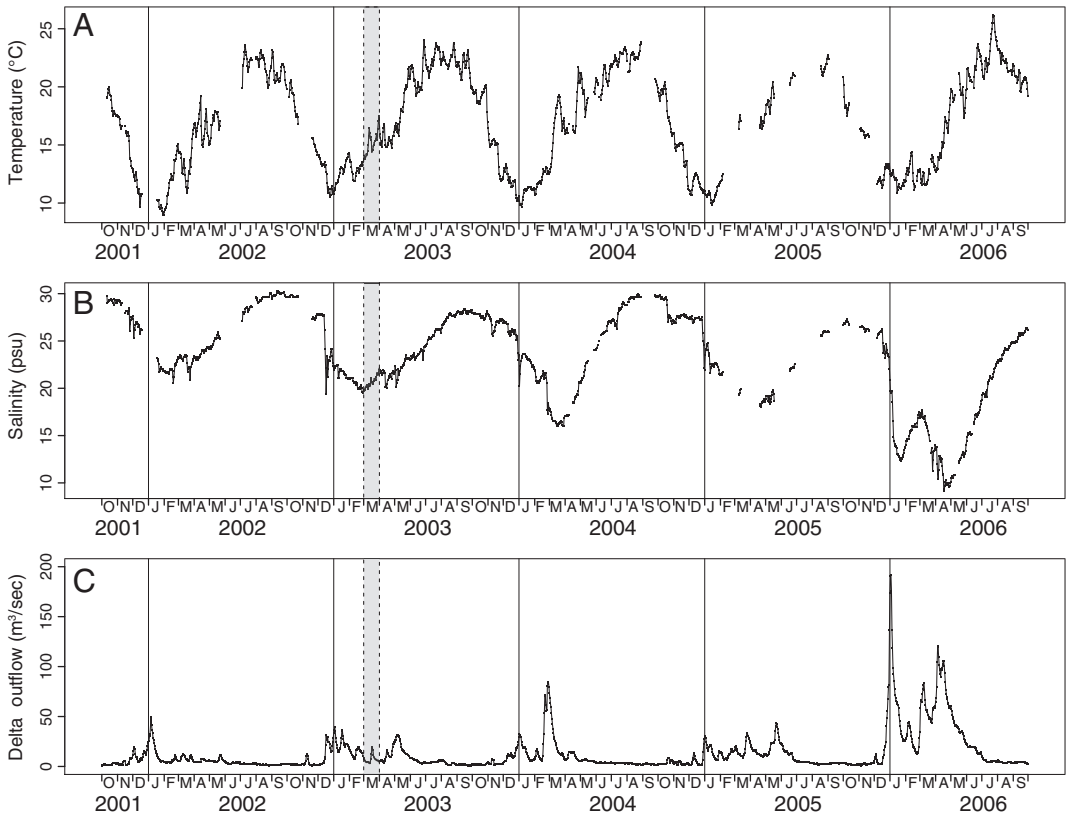

Fig. 1. Environmental data recorded in the San Francisco Bay estuary. A) Average daily temperatures recorded at the USGS gauging station located on the fishing pier adjacent to the eastern end of the Dumbarton Bridge; B) Average daily salinity from the same gauging station; C) Delta outflow recorded by the California Department of Water Resources Interagency Ecological Program. Shaded area marks March 2003.

to the ligamental area and parallel to the growth axis of the resilifer. Twenty-four samples (mass: ~50–100 μg), each approximately 100 μm wide, 200 μm deep, and 1300 μm long, were drilled from OY-003, while twenty-two samples (mass: ~50–100 μg), each approximately 150 μm wide, 200 μm deep, and 1600 μm long, were drilled from OY-018. In both specimens, the micromilled samples represent shell material deposited early in 2003 (~March: see below). Throughout this manuscript, these profiles will be referred to as the "high-resolution" stable isotope profiles.

All carbonate isotopic analyses were performed on a Finnigan MAT 252 mass spectrometer equipped with a Kiel III automated sampling device at the Environmental Isotope Laboratory, Department of Geosciences, University of Arizona. Samples were reacted with >100% orthophosphoric acid at 70°. Results are reported in δ notation (‰) by calibration to the NBS-19 reference standard ($\delta^{13}C = +1.95$‰ VPDB and $\delta^{18}O = -2.20$‰ VPDB). Repeated measurement of standard carbonates resulted in standard deviations of ±0.06‰ and ±0.08‰ for carbon and oxygen, respectively.

2.4. Barium/calcium ratios

Shell Ba/Ca ratios were analyzed using the laser ablation-inductively coupled plasma-mass spectrometer (LA–ICP-MS) facility at Union College (CETAC LSX-213 frequency quintupled Nd:YAG laser ablation unit ($\lambda = 213$ nm) coupled to a Perkin Elmer Elan 6100 DRC ICP-MS). Low-resolution profiles were constructed from samples collected every 200 to 400 μm from the same plane as the high-resolution stable isotope profiles. These profiles represent the majority of the lifespan of the oyster, however, in each specimen, the earliest stages of ontogeny were not sampled (see below). High-resolution samples were collected every 50 to 80 μm from the trough produced during micromilling. For all analyses, ^{138}Ba and ^{43}Ca were monitored. Helium was used as the carrier gas (600 ml/min), which was mixed with argon after the ablation cell (800 ml/min). The ICP-MS was optimized to achieve ThO/Th ratios less than 0.5%. A spot size of 50 μm was used with the laser set at 10 Hz and 600 burst counts. A 15-second pre-ablation interval was used for gas blank corrections. Calibration using the NIST 612 (values from Pearce et al., 1997), including gas blank subtraction and ^{43}Ca normalization, was performed using GeoPro software (CETAC). The USGS standard MACS-3 was used to check the calibration, which suggests a robust LA–ICP-MS calibration and good reproducibility (Ba = 58.6 ± 2.0 ppm, n = 12, RSD = 3.5%, on two analytical days; recommended value = 58.7 ± 2.0 ppm; USGS, 2011). Ba/Ca ratios from the MACS-3 pellet were 42.8 ± 1.5 μmol/mol or 3.5% relative standard deviation (n = 12). This suggests an absolute error of approximately 0.035 to 0.175 μmol/mol for the range of Ba/Ca ratios observed in our shells (i.e., 1 to 5 μmol/mol). Thus we use the conservative estimate of 0.2 μmol/mol for all shell data.

3. Results

3.1. Temperature, salinity, and freshwater input

Fig. 1 shows average daily temperature, salinity, and Delta outflow from October 2001 through September 2006. Goodwin et al. (2010) discussed these records extensively and identified several salient patterns (also see Conomos, 1979 and Schemel et al., 2003 for detailed discussions of temperature and salinity variation in South San Francisco Bay). These include:

1. Strong seasonal variation of temperature and salinity. The average daily water temperature was 16.9 °C. Annual temperature variation was ~12 °C. The warmest temperatures generally occur in

late summer (July and August), while coolest temperatures are recorded in December and January (Fig. 1A). The maximum and minimum temperatures were 26.2 °C (July 24, 2006) and 9.0 °C (January 30 and 31, 2002), respectively. The average daily salinity was 23.5 psu. The highest salinities were recorded in September and October at the end of the hot summer (Fig. 1B). The highest recorded salinities (30.3 psu) were recorded September 12 and 13, 2002 and the lowest salinity value (9.2 psu) occurred on April 18, 2006.

2. Pronounced periods of high Delta outflow in the winter and early spring followed by low flow in the summer months. Episodes of high Delta outflow are consistent with the highly seasonal pattern of precipitation in the Sacramento and San Joaquin catchments (dry summers and wet winters; author's personal observations).
3. Distinctive pattern of inter-annual salinity minima. The lowest salinities were recorded in 2006, when there were two distinct salinity minima, and in 2004, which was characterized by a single minimum. These low salinity events correspond to distinct pulses of Delta outflow (see Conomos, 1979 for general discussion). In 2004, there was one major pulse of Delta outflow, and in 2006 there were two, one in January and the other in April (Fig. 1C).

3.2. Chlorophyll a

Fig. 2 shows a time series of calculated chlorophyll *a* concentrations for USGS stations 30 and 33 in south San Francisco Bay. These data clearly illustrate the prominent spring phytoplankton blooms that characterize San Francisco Bay (Cloern, 1996; Cloern et al., 2007). In general, spring blooms begin in early February, reach maximum [chl *a*] by early March, and wane by early April (e.g., Fig. 3). The time series in Fig. 2 also shows inter-annual [chl *a*] variability. At each location, the highest [chl *a*] were recorded in the spring of 2003, followed by spring 2006 and 2004. While the overall pattern of [chl *a*] is similar, there are significant between-locality variations, even during the same bloom event (also see Cloern, 1996). For example, the 2006 spring bloom shows a bimodal pattern at both stations (Fig. 2A and B). At station 30 (Fig. 2A), however, the initial peak has a [chl *a*] of <40 μg/l and the second peak has chl *a* concentrations of ~50 μg/l, whereas this pattern is reversed further south at station 33 (Fig. 2B).

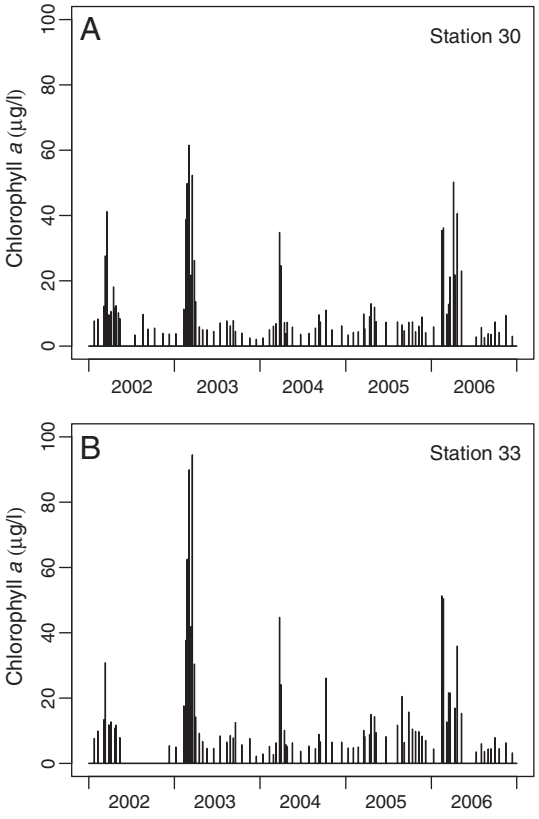

Fig. 2. Calculated chlorophyll *a* concentrations from two sites in south San Francisco Bay. A) USGS Station 30, Redwood Creek: 37° 33.3′ N, 122° 11.4′ W. B) USGS Station 33, Dumbarton Bridge: 37° 30.5′ N, 122° 7.3′ W. See http://sfbay.wr.usgs.gov/access/wqdata for detailed information.

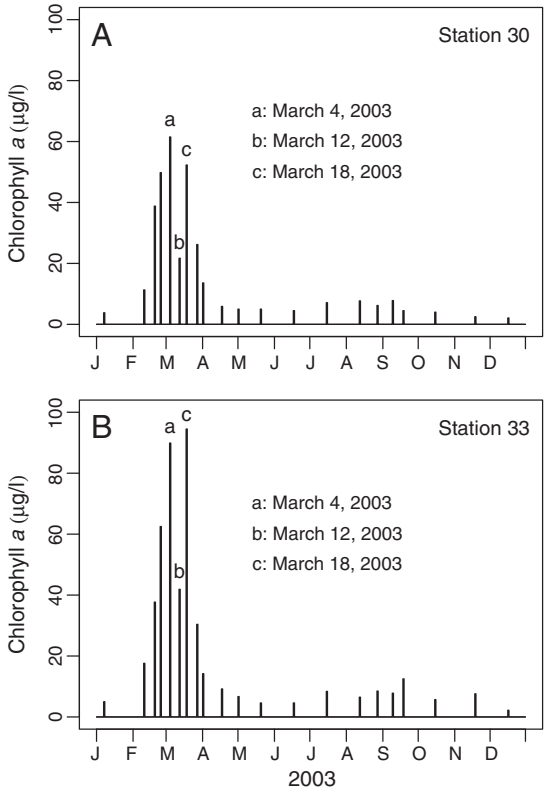

Fig. 3. 2003 calculated chlorophyll *a* concentrations for USGS gauging stations 30 and 33. The dates marked a–c delineate the timing of the bimodal phytoplankton bloom. See text for discussion.

Calculated chlorophyll *a* concentrations for 2003 are shown in Fig. 3. The overall timing and duration of the spring bloom was identical at both locations. The maximum [chl *a*], however, was higher at the southern station. Like the 2006 bloom, the 2003 bloom was bimodal at both locations. At station 30 (Fig. 3A), the first peak (March 4) had the highest concentration (61.5 μg/l), followed by a nadir on March 12, and the second peak on March 18 (52.3 μg/l). At station 33, the March 4th peak had a [chl *a*] of 89.9 μg/l, whereas the second peak had higher concentrations (94.5 μg/l; Fig. 3B).

The spatial and temporal variability shown in Figs. 2 and 3 is characteristic of the well documented phytoplankton bloom system in San Francisco Bay (Cloern, 1996; Cloern et al., 2007; Thompson et al., 2008). In general, turbidity is negatively correlated with phytoplankton abundance. Tidal currents are largely responsible for resuspension and transportation of suspended sediments (Thompson et al., 2008). Cloern (1991) demonstrated that phytoplankton bloom magnitudes are greatest when tidal current velocities are lowest, on or about the vernal equinox (Thompson et al., 2008). This, temporal pattern is amplified by salinity stratification of the water column associated with late winter and early spring Delta outflow (Cloern, 1984). Shorter scale (daily to weekly) variations are a function of vertical mixing of the water column, which in turn, are controlled by wind and the tidal cycle. Cloern (1991) showed that during spring phytoplankton blooms, increases in biomass coincide with neap tides and blooms dissipated during spring tides.

3.3. Stable isotope profiles

The low-resolution $\delta^{18}O$ and $\delta^{13}C$ profiles from specimens OY-018 and OY-003 are shown in Fig. 4A and B, respectively. These data were originally presented in Goodwin et al. (2010). In each specimen, four concave down cycles are present in the $\delta^{18}O$ and $\delta^{13}C$ profiles. In addition, the end of an initial cycle and the beginning of a final cycle are present in the profile from OY-003 (Fig. 4B), whereas only the beginning of a final cycle is present in the profile from OY-018 (Fig. 4A). Using environmental data, Goodwin et al. (2010) demonstrated that these cycles were annual and the oysters were approximately 4.5 years old. Furthermore, because these specimens were collected alive (OY-003: 7/28/06; OY-018: 8/9/06), they likely settled early in 2002. This conclusion is supported by the fact that the predicted $\delta^{18}O_{carb}$ profile, calculated from water temperatures and salinity derived $\delta^{18}O_{water}$ values, closely mimics the observed $\delta^{18}O_{carb}$ cyclicity. Thus, using the predicted $\delta^{18}O_{carb}$ profile as a guide (Goodwin et al., 2010: Fig. 2D), calendar years were placed on the observed $\delta^{18}O_{carb}$ profiles (vertical lines in Fig. 4). The position of the time-lines was chosen because the most positive $\delta^{18}O$ values in the predicted profile always fell immediately before the new year (see Goodwin et al., 2010 for a complete discussion). Furthermore, the inter-annual pattern of salinity minima (Fig. 1B), which reflects Delta outflow (Fig. 1C), is shown in the observed $\delta^{18}O_{carb}$ profiles. That is, 2004 and 2006 saw above average Delta outflows and lower than normal salinity minima. In both OY-003 and OY-018, the minimum $\delta^{18}O_{carb}$ values in 2004 and 2006 were lower than the minimum values in years with average salinity minima or Delta outflows. In addition, 2006 was wetter than 2004 and in both shells the minimum $\delta^{18}O_{carb}$ values in 2006 were lower than 2004 despite ontogenetic amplitude attenuation (sensu Goodwin et al., 2003). Finally, in both shells the $\delta^{13}C$ profiles are marked by a prominent "carbon spike" in shell deposited early in 2003. This chronology also suggests that a prominent "carbon spike," which is present in the $\delta^{13}C$ profiles from each specimen, was deposited early in 2003. This conclusion is supported by at least five different specimens (see Goodwin et al., 2003). These "carbon spikes" likely correlate with the largest spring phytoplankton bloom in south San Francisco Bay between 2002 and 2006 (Fig. 2).

High-resolution $\delta^{18}O$ and $\delta^{13}C$ profiles (Fig. 5) were micromilled from the same region of the shell represented by the "carbon spike" in the low-resolution profile and, therefore, also correlate with the 2003 spring phytoplankton bloom. Using growth bands and growth increments (sensu Richardson, 2001), the low- and high-resolution profiles were aligned: The vertical arrows in Fig. 5A and B mark the location of the "carbon spike" from the low-resolution profile.

The $\delta^{18}O$ profiles from each shell show a similar pattern. Values descend from an initial value of approximately −0.5‰ to minimum values around −3.5‰. This pattern mimics the overall variation in the low-resolution oxygen isotope profiles from early 2003 (Fig. 4A and B). The high-resolution $\delta^{13}C$ profiles clearly show the "carbon spike." The profile from OY-003 represents the entire spike, whereas the data from OY-018 fails to capture the minimum values following the positive excursion. The $\delta^{13}C$ profile from OY-003 (Fig. 5B) has a broad, flat peak with two distinct bumps, while the OY-018 has a sharp peak and an asymmetrical shape.

3.4. Barium/calcium profiles

Low-resolution Ba/Ca profiles from OY-018 and OY-003 are shown in Fig. 4A and B, respectively. The profiles from each specimen are characterized by relatively constant background values (~1 μmol/mol) interrupted by distinct, periodic peaks and are reminiscent of previously documented Ba/Ca profiles (Stecher et al., 1996; Vander Putten et al., 2000; Lazareth et al., 2003; Gillikin et al., 2006b; Gillikin et al., 2008; Thébault et al., 2009). Each Ba/Ca data point was sclerochronologically calibrated with the low-resolution $\delta^{18}O$ samples using visible timelines in the shell (Fig. 4). Because these samples were collected from different planes in the shell (see above), we estimate that the error of this sclerochronologic calibration is approximately 1 mm. Nevertheless, the calendar years placed on the stable isotope profiles by Goodwin et al. (2010) can be used to date the Ba/Ca profile. In both profiles,

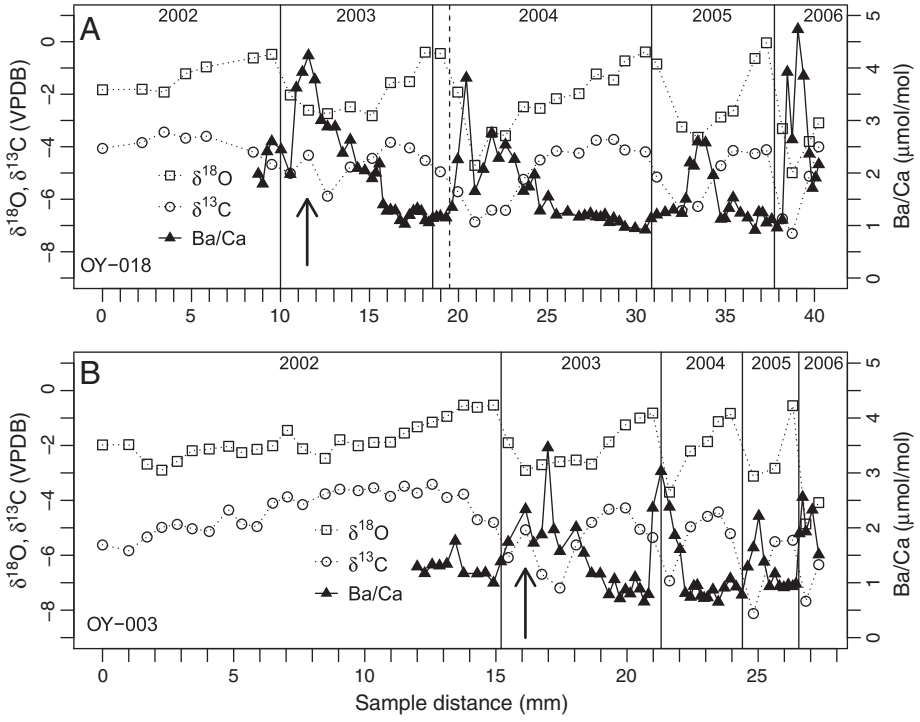

Fig. 4. $\delta^{18}0$, $\delta^{13}C$, and Ba/Ca ratios from two specimens of *Crassostrea gigas* collected from San Francisco Bay. Isotope data from Goodwin et al. (2010). A) Specimen OY-018 collected alive on August 9, 2006 from Hayward Landing. B) Specimen OY-003 collected alive on July 28, 2006 from Dumbarton Bridge. The solid vertical lines, which separate samples into calendar years, were located using predicted $\delta^{18}O_{carb}$ values. Arrows mark the position of the "carbon spike."

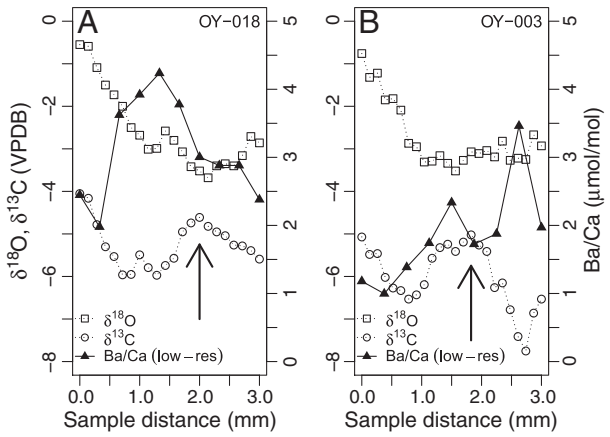

Fig. 5. High-resolution (micromilled) $\delta^{18}O$ and $\delta^{13}C$ from shell deposited during the 2003 spring phytoplankton bloom. Low-resolution Ba/Ca profiles are also shown. This is a subset of the data presented in Fig. 4. Arrows mark the physical position of the "carbon spike" in the low-resolution $\delta^{13}C$ profile (see Fig. 4).

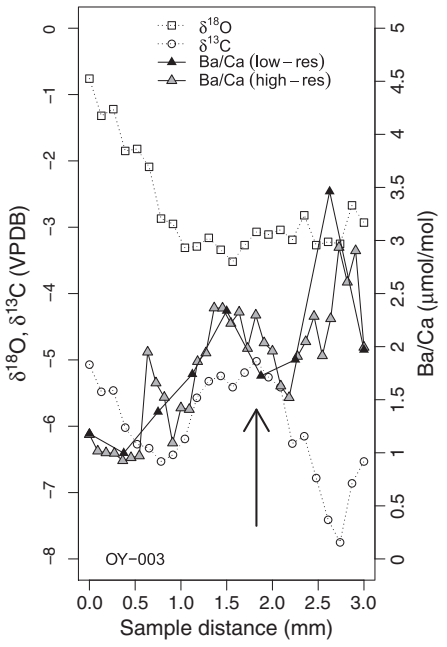

Fig. 6. $\delta^{18}O$, $\delta^{13}C$, and Ba/Ca ratios from OY-003 collected alive on July 28, 2006 from the east end of Dumbarton Bridge in south San Francisco Bay. The "carbon spike," which correlates with the 2003 spring phytoplankton bloom is clearly visible in the $\delta^{13}C$ profile. The arrow marks the physical position of the "carbon spike" from the low-resolution profile.

the peaks occur in shell material deposited in the late winter or early spring, suggesting that the peaks recur annually. Furthermore, the peaks coincide with $\delta^{18}O$ minima (notably in the spring of 2004 and 2006), which represent times of high freshwater input to the estuary.

Despite the gross similarity in the timing of Ba/Ca peaks between the specimens, there are significant differences. First, the peak heights in OY-018 are generally higher than OY-003: Three of the four peaks from OY-018 are between 3.8 and 4.7 μmol/mol, whereas the highest peak from OY-003 is 3.4 μmol/mol. Second, the rank order of peak heights differs. In OY-018, 2006 has the highest Ba/Ca value followed by 2003, 2004 and 2005. In OY-003, however, the highest value was recorded in 2003 and then 2004, 2006, and finally 2005. Third, the exact timing of the peaks is different. For example, in OY-018, the 2004 Ba/Ca peak begins after the new year (Fig. 4A). Even if a less conservative estimate for the end of year is used (dotted line in Fig. 4A), the peak does not begin until 2004. In OY-003, the correlative peak begins in shell material dated from 2003 and clearly begun earlier. Finally, the shapes of correlative peaks differ between specimens. For example, in 2003 the peak from OY-003 has a symmetrical shape with a main central peak flanked on either side by a single smaller peak. In contrast, the peak from OY-018 is not symmetrical and no distinct peak is present to the right of the main peak. Similarly, in 2006, both profiles are bimodal although the rank order of the local maxima is reversed (Fig. 4).

The high-resolution Ba/Ca profile from OY-003 is shown in Fig. 6. The high-resolution profile (gray triangles) shows a similar overall pattern of variation to the low-resolution profile (black triangles). In the low-resolution profile, initial values rise from ~1 μmol/mol to between 2 and 4 μmol/mol. This overall increasing trend is interrupted by two peaks one at sample distance 1.5 mm and another at 2.6 mm. These peaks are also present in the high-resolution profile, although in each case there is more high-frequency variation. In addition, the peak located at 0.6 mm in the high-resolution profile is not present on the low-resolution profile.

4. Discussion

4.1. Stable isotope profiles

The calibration of the "carbon spike" with the 2003 spring phytoplankton bloom, suggests that it reflects changes in the local aqueous geochemical system associated with photosynthetic activity. During a phytoplankton bloom, autotrophic production results in high $\delta^{13}C_{DIC}$ values as plankton remove ^{12}C from the water faster than ^{13}C (Fogel and Cifuentes, 1993). Spiker and Schemel (1979) showed that in north SFB, relatively high $\delta^{13}C_{DIC}$ values coincide with increases in [chl *a*]. Similarly, Coffin and Cifuentes (1999) showed that, in the Perdido Estuary (Florida, USA), during periods of elevated phytoplankton production, $\delta^{13}C_{DIC}$ values were higher than expected, and Gillikin et al. (2006b) illustrated a similar relationship in the Scheldt Estuary (Netherlands). This link has also been documented in both fully marine settings (e.g. Tamelander et al., 2009) and freshwater habitats (authors' personal observations; also see Parker et al., 2010). To definitively link the 2003 spring phytoplankton bloom with the "carbon spike," however, we would ideally have paired [chl *a*] and $\delta^{13}C_{DIC}$ samples. Unfortunately, we do not have information on the isotopic composition of DIC in south SFB during 2003. Therefore, we need to examine other potential controls on $\delta^{13}C_{DIC}$.

DIC in estuaries is derived from multiple sources with different $\delta^{13}C$ values. In general, the marine end member has a $\delta^{13}C$ value close to 0‰, whereas freshwater has more negative values (Mook and Tan, 1991). In SFB, freshwater input via the delta has a $\delta^{13}C_{DIC}$ value of approximately −10‰, whereas the marine end member is ~+2‰ (Spiker and Schemel, 1979). If the "carbon spike" reflects changes in the ratio of these end members, less freshwater from the delta should have penetrated into south SFB (see Conomos, 1979). Alternatively, freshwater input from small intermittent streams (approximately 10% of annual input; Conomos, 1979) could have decreased. These scenarios are unlikely, however, given that the 2003 spring bloom occurred in February and March (Fig. 3) when delta outflow was relatively high and salinity was at or near it its lowest values for the year (Fig. 1C and B, respectively). DIC isotopic values can also be influenced by CO_2 gas exchange with the atmosphere. Preferential degassing of $^{12}CO_2$ to the atmosphere results in enrichment of ^{13}C in the DIC pool. Spiker (1980) showed that annual CO_2 flux to the atmosphere together with net photosynthesis in SFB is balanced by remineralization of organic matter. During spring phytoplankton blooms, however, primary production exceeds respiration (Cloern, 1996), leading to a ^{13}C-rich DIC pool. Remineralization of in situ organic matter can also influence $\delta^{13}C_{DIC}$ by releasing ^{12}C-enriched CO_2. To have caused the observed "carbon spike," remineralization of organic matter should have

temporarily slowed during an interval of enhanced phytoplankton activity (i.e., the spring of 2003). Numerous studies, however, have shown that in systems like the SFB estuary, where phytoplankton are a dominant source of labile organic matter, primary productivity is highly correlated with heterotrophic consumption (see Cloern, 1996 and references therein). Thus, decreased microbial metabolic activity seems an unlikely cause for the "carbon spike."

The "carbon spike" could reflect a change in the ratio of metabolic carbon (i.e., the oyster's respired CO_2) to environmental carbon (DIC) used during biomineralization. Lorrain et al. (2004) showed that in *Pectin maximus* shells, the percentage of metabolic C increases through ontogeny, likely reflecting increased soft tissue mass. In a model recently proposed by Chauvaud et al. (2011), sub-annual changes in food availability were linked to the $\delta^{13}C_{carb}$ through the $C_{metaboloc}/C_{DIC}$ ratio. They demonstrated that episodes of elevated food availability, consisting mainly of ^{12}C-enriched diatoms, are correlated with decreased $\delta^{13}C_{carb}$ values. Unlike these negative $\delta^{13}C_{carb}$ events however, the "carbon spike" in the *Crassostrea gigas* specimens from SFB is a positive excursion. One potential reason for this difference may reflect decoupling of surface waters from the sediment water interface. The specimens used by Chauvaud et al. (2011) were collected from normal marine waters, at least 20 m deep, on the continental shelf. In these settings, the water column is generally well mixed and would tend to dilute photosynthetically ^{13}C-enriched DIC (especially at the surface), while leaving ^{12}C-enriched POM behind in the water column. In turn, this POM sinks to the bottom to be consumed by benthic bivalves. In contrast, the average depth of SFB is ~4 m, and the specimens used in this study were collected from the intertidal zone. Thus, they were likely calcifying in water with relatively high $\delta^{13}C_{DIC}$ values. Furthermore, in south SFB, background $\delta^{13}C_{POM}$ values generally fall between −27‰ and −23‰, while during spring phytoplankton blooms, $\delta^{13}C_{POM}$ values can increase to −18‰ to −17‰ (Cloern, 1996). The carbon isotope values of tissues from the invasive bivalve *Potamocorbula amurensis* living in south SFB show a similar pattern. Most of the year, $\delta^{13}C_{tissue}$ values reflect background POM values, however, during the spring bloom, when phytoplankton dominate the POM, $\delta^{13}C_{tissue}$ values increase to −17‰ (Cloern, 1996). Thus, during the 2003 spring phytoplankton bloom in south SFB $\delta^{13}C_{DIC}$, $\delta^{13}C_{POM}$, and likely δ^{13}C of oyster tissue were trending to more positive values. Taken together, these data support the hypothesis that the "carbon spike" reflects photosynthetic enrichment of the DIC pool in ^{13}C.

Phytoplankton blooms begin when algal concentrations rise above background levels. In the southern reaches of SFB, typical chl *a* concentrations are <10 μg/l (Cloern, 1996). The 2003 spring bloom began no later than February 10, ending on or after April 1, and lasted at least 51 days. In the low-resolution δ^{13}C profiles, the 2003 bloom is represented by a single sample (arrows in Fig. 4A and B). In the high-resolution profiles (Fig. 5A and B), the same event is represented in OY-018 and OY-003 by 13 and 16 samples, respectively. Assuming a constant growth rate during this interval, the temporal resolution of the high-resolution samples from OY-018 and OY-003 are approximately 3.9 and 3.2 days/sample, respectively. The profile from OY-018, however, does not capture the entire bloom and therefore 3.9 days/sample is likely a conservative estimate. Nevertheless, because the temporal resolution of the isotope samples is greater than the calculated chl *a* samples, their variation may reflect changes in [chl *a*]. Because we do not have $\delta^{13}C_{DIC}$ samples, however, we used $\delta^{18}O_{carb}$ samples to calibrate $\delta^{13}C_{carb}$ with [chl *a*] variation.

Fig. 7 shows temperature and salinity at Dumbarton Bridge for March, 2003. Between March 4 and 18 waters warmed by ~3 °C and then cooled back to its original temperature (Fig. 7A). During the same interval salinity remained relatively constant (Fig. 7B). Together, these data suggest that carbonate deposited in early to middle March should be characterized by a negative δ^{18}O excursion of approximately 0.5‰. Fig. 8A shows predicted daily $\delta^{18}O_{carb}$ values for shell carbonate deposited at Dumbarton Bridge in March 2003 (see

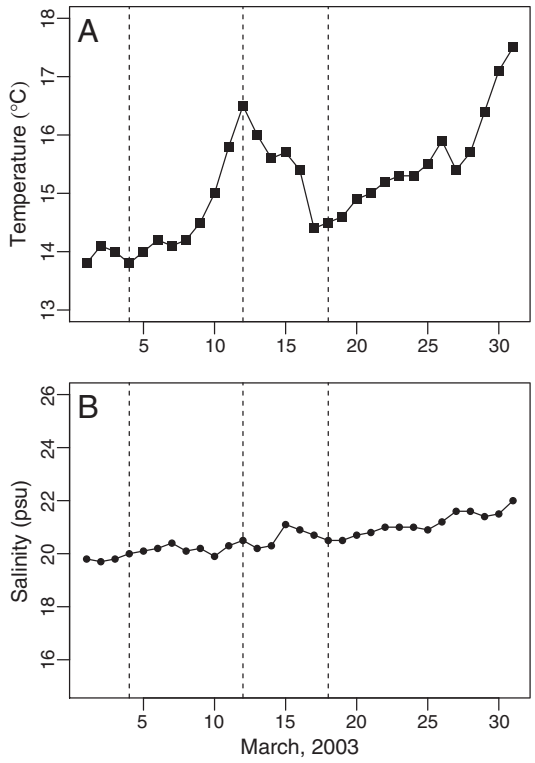

Fig. 7. Average daily temperature (A) and salinity (B) for March 2003 from the USGS gauging station at the eastern end of the Dumbarton Bridge. March 4, 12 and 18 are marked by vertical dashed lines.

Goodwin et al., 2010 for details). The ^{18}O enrichment event is clearly visible and centered on March 12, the warmest day between March 4 and 18. Fig. 8A also shows the average of each successive set of three samples (filled circles), the resolution of the micromilled samples from OY-003. Fig. 8B shows the micromilled $\delta^{18}O_{carb}$ samples that correlate with the most positive portion of the "carbon spike" from OY-003 (samples 10–19 in Fig. 5B). These samples show the same pattern of variation as at the predicted $\delta^{18}O_{carb}$ profile, however, they are consistently approximately 1‰ more positive. Goodwin et al. (2010) discussed reasons for this offset extensively, they include: 1) uncertainty in the salinity–δ^{18}O relationship; 2) local environmental variation within SFB; 3) potential recent environmental change, and; 4) isotope sample resolution (see also Goodwin et al., 2001). Nevertheless, because the offset is consistent and the overall pattern between the predicted and observed profiles is so similar, we adjusted the observed $\delta^{18}O_{carb}$ profile by subtracting 1‰ from each value (Fig. 8C). The close match between these profiles suggests that the micromilled samples represent 3-day averages of March environmental conditions. Furthermore, the most negative $\delta^{18}O_{carb}$ value in the micromilled profile (−3.52‰; sample distance: 1.6 mm) was precipitated between March 11 and 13, 2003.

Using this relationship as a pinning point, it is possible to calibrate $\delta^{13}C_{carb}$ and [chl *a*] variation. The 2003 spring phytoplankton bloom was characterized by bimodal calculated chl *a* concentrations (Fig. 3). At Station 33, the highest [chl *a*] occurred on March 18, while the next highest was measured on March 4 (Fig. 3B). These elevated chl *a* concentrations were separated by much lower value measured on March 12. Similarly, the δ^{13}C profile from OY-003 is bimodal and the second peak is higher than the first (Fig. 5B). The minimum value that separates the peaks is the same sample used to date the δ^{18}O profile, which was deposited on March 11–13. Accordingly, the most positive value in the $\delta^{13}C_{carb}$ profile (−5.02‰; Fig. 5B: sample distance: 1.8 mm) was deposited on March 17–19 when [chl *a*] at Station 33 was highest. The second highest [chl *a*] value was measured on March 4 and correlates

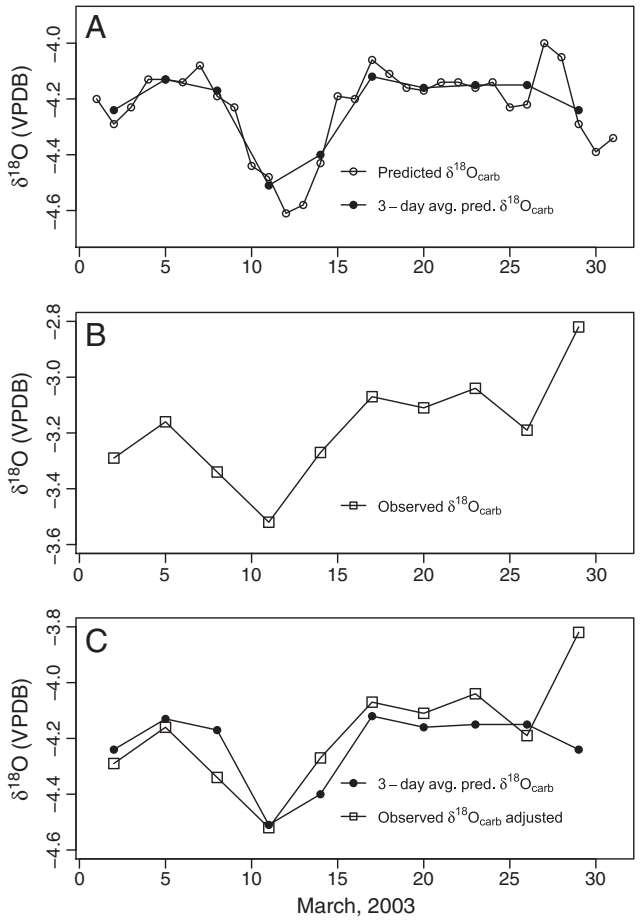

Fig. 8. A) Predicted daily $\delta^{18}O_{carb}$ values for shell carbonate deposited at Dumbarton Bridge in March 2003. Also shown is the average of each successive set of three samples. B) Micromilled $\delta^{18}O_{carb}$ samples that correlate with the most positive portion of the "carbon spike" from OY-003 (samples 10–19 in Fig. 5B). C) Three-day average predicted $\delta^{18}O_{carb}$ values from A, and micromilled $\delta^{18}O_{carb}$ samples from B. The micromilled sampled have been adjusted by subtracting 1‰ from each value. See text for discussion.

with the 10th sample (−5.57‰; Fig. 5B: sample distance: 1.2 mm). These data suggest that sub-weekly variations in [chl *a*] are reflected in $\delta^{13}C_{carb}$ variation. While the difference in peak heights (0.3‰; peak 1: −5.32‰, 1.4 mm; peak 2: −5.02‰, 1.8 mm) is close to machine error, the peaks are superimposed on a declining baseline (Fig. 5B), suggesting that the $\delta^{13}C_{carb}$ offset is likely even greater. Thus, $\delta^{13}C_{carb}$ variation may be able to resolve relatively small differences in [chl *a*].

Because the "carbon spike" from OY-018 does not capture the entire bloom, it is more difficult to calibrate $\delta^{13}C_{carb}$ with [chl *a*] variation. Furthermore, because we do not have water temperatures or salinities from Hayward Landing, we cannot directly relate oxygen isotopes with environmental variation. Nevertheless, a pronounced negative excursion centered on 2.1 mm is present in the $\delta^{18}O$ profile (Fig. 5A). Assuming this excursion represents the same warming event that took place farther south at Dumbarton Bridge, the sample with the most negative $\delta^{18}O$ value (−3.68‰) was deposited on or around March, 12. The most positive $\delta^{13}C_{carb}$ value in the "carbon spike" (−4.41‰) was measured from the preceding sample, which most likely correlates with the highest [chl *a*] measured at Station 33 on March 4. It is somewhat surprising that the second peak, correlating to the March 18 spike in [chl *a*], is not present in the $\delta^{13}C_{carb}$ profile. Assuming the profile is dated correctly, this suggests a threshold below which high-frequency variations in [chl *a*] and subsequent $\delta^{13}C_{DIC}$ changes are not recorded in shell carbonate.

Taken together, these data highlight the potential utility of stable isotope records as tools for reconstructing patterns of primary productivity. The 2003 spring phytoplankton bloom is clearly visible in the low- and high-resolution carbon isotope profiles from specimens living at each locality (Figs. 4 and 5). At low concentrations, high-frequency [chl *a*] variations do not appear to be recorded. When [chl *a*] is high, however, $\delta^{13}C_{carb}$ profiles qualitatively reflect [chl *a*] variation with 3-day resolution. While we do not have $\delta^{13}C_{DIC}$ data nor do we know the percentage of metabolic carbon incorporated into the shell, our findings suggest that it should be possible to calibrate $\delta^{13}C_{carb}$ variation with [chl *a*] to develop a quantitative phytoplankton proxy. This seems to be a promising future research direction, especially in shallow coastal estuaries like SFB.

4.2. Barium/calcium profiles

The Ba/Ca profiles from OY-018 and OY-003 are characterized by relatively constant background values, punctuated by distinct, periodic peaks (Fig. 4). Sclerochronological calibration with the stable isotope profiles suggests that these Ba/Ca peaks are recorded each year in the spring. Thus, like stable isotopes, the Ba/Ca profiles from these specimens can be used to demarcate individual years of shell growth. That said, elevated spring Ba/Ca values are not always recorded in shell carbonate, even in specimens living in environments with significant levels of spring primary productivity (e.g.,. Barats et al., 2009), and extrapolating our findings to other specimens should be done with caution. Nevertheless, the regular cyclicity of these profiles suggests that they are deposited in response to an annual environmental forcing (Gillikin et al., 2008; Thébault et al., 2009).

Recent studies have linked Ba/Ca ratios in biogenic carbonates with several environmental variables (Thébault et al., 2009). Gillikin et al. (2006b), for example, showed that in the mussel *Mytilus edulis*, background $(Ba/Ca)_{carb}$ is directly proportional to $(Ba/Ca)_{water}$. The low-resolution Ba/Ca profiles from the specimens examined here have relatively constant background values (Fig. 4). If the relationship described by Gillikin et al. (2006b) holds for *C. gigas*, dissolved Ba concentrations in south SFB remained relatively constant between 2003 and 2006.

Numerous studies have also suggested a link between phytoplankton blooms and Ba/Ca peaks in shells (e.g., Vander Putten et al., 2000; Lazareth et al., 2003; Thébault et al., 2009). Gillikin et al. (2008), on the other hand, disputed this hypothesis, suggesting that an as yet unknown mechanism was responsible for Ba/Ca peaks in biogenic carbonates. If the Ba/Ca ratios were a function of phytoplankton abundance, we would expect them to correlate with chl *a* concentrations. Fig. 4 shows the low-resolution Ba/Ca profiles, which have been sclerochronologically calibrated with the stable isotope profiles. The highest Ba/Ca values measured from the OY-018 in 2003 coincides with the "carbon spike." The first samples in the profile, however, are between 2 and 3 μmol/mol, well above the background values, suggesting that elevated Ba/Ca ratios may have predated the carbon spike. Similarly, in OY-003 a Ba/Ca peak correlates with the "carbon spike." The highest Ba/Ca value, however, was measured from carbonate deposited well after the most positive $\delta^{13}C$ value. Because only the 2003 bloom was recorded in the $\delta^{13}C$ profiles we cannot conduct similar comparison in the subsequent years. Nevertheless, given the synchrony of blooms in SFB (Cloern, 1996), and the mismatch in the timing of Ba/Ca peaks in 2004, 2005, and 2006, the link with phytoplankton blooms is dubious. Finally, if Ba/Ca ratios were recording bloom magnitude, we would expect the rank order of peak heights to correlate with spring bloom chl *a* concentrations. However, not only do the rank orders of annual peak magnitudes differ between specimens (Fig. 4), but neither Ba/Ca profile matches bloom magnitudes (Fig. 2).

Calibration of the low-resolution Ba/Ca profiles with the high-resolution (micromilled) isotope samples also casts doubt on this

connection (Fig. 5). Recall that both sets of samples were collected from the same location, on a plane cut perpendicular to the ligamental area. Their calibration, therefore, is likely more accurate than between the low-resolution Ba/Ca profiles and the hand-drilled isotope samples (Fig. 4). In OY-018 (Fig. 5A), Ba/Ca ratios and $\delta^{13}C$ values are out of phase. The highest Ba/Ca value measured from 2003 (4.2 μmol/mol), was deposited about the same time the bloom began. Furthermore, Ba/Ca ratios decline continuously as the bloom waxes and wanes throughout February and March.

The low-resolution Ba/Ca ratios marking the 2003 spring bloom in OY-003 show a somewhat different pattern (Fig. 5B). Increasing $\delta^{13}C$ values, marking the initial phase of the bloom, coincide with increasing Ba/Ca values. However, at the height of the bloom (March, 18), marked by the most positive $\delta^{13}C$ value, Ba/Ca ratios had declined. Finally, as $\delta^{13}C$ values decreased, marking the final phase of the bloom, Ba/Ca ratios rose to the highest values recorded in OY-003. The high-resolution Ba/Ca profile from OY-003 shows a similar pattern (Fig. 6). Like the low-resolution profile, it is marked by an overall increasing trend. The "carbon spike" is marked by a distinct spike in Ba/Ca values. However, troughs in the $\delta^{13}C$ profile immediately before and after the "carbon spike" coincide with relatively high Ba/Ca ratios.

These data suggest that the Ba/Ca ratios do not correlate with [chl *a*] in south SFB. Nevertheless, there does seem to be a pacemaker responsible for their deposition. As discussed above, Gillikin et al. (2006b) showed that background $(Ba/Ca)_{carb}$ values are directly proportional to $(Ba/Ca)_{water}$. Because freshwater has higher Ba/Ca ratios than marine waters (Coffey et al., 1997; Gillikin et al., 2006b), Ba/Ca peaks may be correlated with freshwater discharge. While the timing of Ba/Ca peaks in our specimens is loosely correlated with Delta outflow—both occur in the late winter and early spring—specimens living in fully marine environments, not influenced by freshwater input, also exhibit spring Ba/Ca peaks (Gillikin et al., 2008; Barats et al., 2009). Moreover, were our Ba/Ca peaks a function of Delta discharge, the largest peaks would have occurred in 2004 and 2006 when salinities were lowest and Delta outflows were highest (Fig. 1B and C, respectively). Ba/Ca peak magnitudes, however, do not show this pattern. Furthermore, in each year, significant Delta outflow had begun by early January (Fig. 1C). In OY-003, however, the 2005 Ba/Ca peak is correlated with the lowest $\delta^{18}O_{carb}$ values (Fig. 4B), which were likely deposited in May (see Goodwin et al., 2010). Gillikin et al. (2006b) speculated that Ba/Ca peaks might reflect selective feeding on Ba-rich phytoplankton species or changes in the relative abundance of Ba-rich taxa during bloom events. However, we cannot test these hypotheses here. Thus, while it is clear that abundant hypotheses exist, for the time being, the exact cause of Ba/Ca peaks in biogenic carbonates remains unknown.

5. Conclusions

Here we present high-resolution geochemical profiles from two potential productivity proxy systems archived in shells of the oyster *Crassostrea gigas*. We used to oxygen isotopes variation in shell carbonate to establish inter- and intra-annual chronologies. In turn, we used these chronologies to compare $\delta^{13}C_{carb}$ and $(Ba/Ca)_{carb}$ variations with inter- and intra-annual records of environmental variation. The following conclusions were reached based on these comparisons:

1. Sclerochronological calibration of the positive $\delta^{13}C_{carb}$ excursion with the 2003 spring phytoplankton bloom, suggests that the "carbon spike" reflects photosynthetic ^{13}C enrichment of the dissolved inorganic carbon pool.
2. Calibrations of the "carbon spike" with elevated chl *a* concentrations during the 2003 spring phytoplankton bloom, suggest that our micromilling sampling strategy is capable of reconstructing environmental variation with three- to four-day resolution during this interval.
3. Calibration of observed $\delta^{18}O_{carb}$ samples with predicted $\delta^{18}O_{carb}$ values, calculated from water temperatures and salinity derived $\delta^{18}O_{water}$ values, suggests that the high-resolution $\delta^{13}C_{carb}$ profile can be directly related to [chl *a*]. This finding highlights the potential utility of stable isotope records as tools for reconstructing patterns of primary productivity.
4. Sclerochronological calibration of Ba/Ca profiles with stable isotopes suggest that elevated Ba/Ca values are recorded each year in the spring. Thus, like stable isotope, the Ba/Ca profiles from these specimens can be used to demarcate individual years of shell growth. That said, extrapolating our findings to other specimens should be done with caution.
5. Ba/Ca ratios do not correlate with the 2003 spring phytoplankton bloom. Furthermore, given the synchrony of blooms and the mismatch in the timing of Ba/Ca peaks, the link with phytoplankton blooms is dubious.
6. Low- and high-resolution Ba/Ca profiles, sampled from the same region of the shell, show a similar overall pattern of variation. Differences, in the profiles, however, cast further doubt on the relationship between Ba/Ca and phytoplankton blooms. Moreover, Ba/Ca profiles do not match the pattern of Delta discharge. While they are likely deposited in response to environmental variation, the exact cause of Ba/Ca peaks in biogenic carbonates remains unknown.
7. The San Francisco Bay estuary is an ideal environment in which to further investigate the relationship between skeletal geochemical variation and patterns of primary productivity.

Acknowledgments

We thank Andy Cohen for proving access to the specimens. Thanks to Ken Bixler, David Dettman, Holli Frey, Sarah Grannemann, Matt Kretchmar, Jessen Havill, and Kurt Hollocher for assistance through the course of this project. DHG acknowledges support provided by the Robert C. Good Faculty Fellowship program at Denison University. DHG also thanks Mary Droser and Nigel Hughes for providing such a hospitable home-away-from-home while on sabbatical. This manuscript benefitted from the thoughtful comments and constructive criticisms of two anonymous reviewers. Finally, we thank the U.S. National Science Foundation for providing funding for the CETAC LSX-213 (NSF-MRI #1039832).

References

Barats, A., Amouroux, D., Chauvaud, L., Pécheyran, C., Lorrain, A., Thébault, J., Church, T.M., Donard, O.F.X., 2009. High frequency Barium profiles in shells of the Great Scallop *Pecten maximus*: a methodical long-term and multi-site survey in Western Europe. Biogeosciences 6, 157–170.

Carré, M., Bentaleb, I., Bruguier, O., Ordinola, E., Fontugne, M., 2006. Calcification rate influence on trace elements incorporation in marine bivalve aragonite: evidences and mechanisms. Geochimica et Cosmochimica Acta 70, 4906–4920.

Chauvaud, L., Thébault, J., Clavier, J., Lorrain, A., Strand, Ø., 2011. What's hiding behind ontogenetic $\delta^{13}C$ variations in mollusk shells? New insights from the giant scallop (*Pectin maximus*). Estuaries and Coasts 34, 211–220.

Cloern, J.E., 1984. Temporal dynamics and ecological significance of salinity stratification in an estuary (south San Francisco Bay, USA). Oceanologica Acta 7, 137–141.

Cloern, J.E., 1991. Tidal stirring and phytoplankton bloom dynamics in an estuary. Journal of Marine Research 49, 203–221.

Cloern, J.E., 1996. Phytoplankton bloom dynamics in coastal ecosystems: a review with some general lessons from sustained investigation of San Francisco Bay, California. Reviews of Geophysics 34, 127–168.

Cloern, J.E., Jassby, A.D., Thompson, J.K., Hieb, K.A., 2007. A cold phase of the East Pacific triggers new phytoplankton blooms in San Francisco Bay. Proceedings of the National Academy of Sciences 104, 18561–18565.

Coffey, M., Dehairs, F., Collette, O., Luther, G., Church, T., Jickells, T., 1997. The behaviour of dissolved barium in estuaries. Estuarine, Coastal and Shelf Science 45, 113–121.

Coffin, R.B., Cifuentes, L.A., 1999. Stable isotope analysis of carbon cycling in the Perdido Estuary, Florida. Estuaries 22, 917–926.

Conomos, T.J., 1979. Properties and circulation of San Francisco Bay Waters. In: Conomos, T.J. (Ed.), San Francisco Bay: The Urbanized Estuary. Pacific Division: American Association for the Advancement of Science, San Francisco, pp. 47–84.

Conomos, T.J., Smith, R.E., Peterson, D.H., Hager, S.W., Schemel, L.E., 1979. Processes affecting seasonal distributions of water properties in the San Francisco Bay

estuarine system. In: Conomos, T.J. (Ed.), San Francisco Bay: The Urbanized Estuary. Pacific Division: American Association for the Advancement of Science, San Francisco, pp. 115–142.
Dettman, D.L., Lohmann, K.C., 1995. Microsampling carbonates for stable isotope and minor element analysis: physical separation of samples on a 20 micrometer scale. Journal of Sedimentary Research A65, 566–569.
Epstein, S., Buchsbaum, R., Lowenstam, H.A., Urey, H.C., 1953. Revised carbonate-water isotopic temperature scale. Bulletin of the Geological Society of America 64, 1315–1326.
Fogel, M.L., Cifuentes, L.A., 1993. Isotopic fractionation during primary production. In: Engel, M., Macko, S.A. (Eds.), Organic Geochemistry. Plenum Press, New York, pp. 73–98.
Fritz, P., Poplawski, S., 1974. ^{18}O and ^{13}C in the shells of freshwater mollusks and their environments. Earth and Planetary Science Letters 24, 91–98.
Gillikin, D.P., De Ridder, F., Ulens, H., Elskens, M., Keppens, E., Baeyens, W., Dehairs, F., 2005. Assessing the reproducibility and reliability of estuarine bivalve shells (*Saxidomus giganteus*) for sea surface temperature reconstruction: implications for paleoclimate studies. Palaeogeography, Palaeoclimatology, Palaeoecology 228, 70–85.
Gillikin, D.P., Lorrain, A., Bouillon, S., Willenz, P., Dehairs, F., 2006a. Stable carbon isotopic composition of *Mytilus edulis* shells: relation to metabolism, salinity $\delta^{13}C_{DIC}$ and phytoplankton. Organic Geochemistry 37, 1371–1382.
Gillikin, D.P., Dehairs, F., Lorrain, A., Steenmans, D., Baeyens, W., André, L., 2006b. Barium uptake into the shells of the common mussel (*Mytilus edulis*) and the potential for estuarine paleo-chemistry reconstruction. Geochimica et Cosmochimica Acta 70, 395–407.
Gillikin, D.P., Lorrain, A., Meng, L., Dehairs, F., 2007. A large metabolic carbon contribution to the $\delta^{13}C$ record in marine aragonitic bivalve shells. Geochimica et Cosmochimica Acta 71, 2936–2946.
Gillikin, D.P., Lorrain, A., Paulet, Y.-M., André, L., Dehairs, F., 2008. Synchronous barium peaks in high-resolution profiles of calcite and aragonite marine bivalve shells. Geo-Marine Letters 28, 351–358.
Goodwin, D.H., Flessa, K.W., Schöne, B.R., Dettman, D.L., 2001. Cross-calibration of daily growth increments, stable isotope variation, and temperature in the Gulf of California bivalve mollusk *Chione cortezi*: implications for paleoenvironmental analysis. Palaios 16 (4), 387–398.
Goodwin, D.H., Schöne, B.R., Dettman, D.L., 2003. Resolution and fidelity of oxygen isotopes as paleotemperature proxies in bivalve mollusk shells: models and observations. Palaios 18 (2), 110–125.
Goodwin, D.H., Cohen, A.C., Roopnarine, P.D., 2010. Forensics on the half shell: a sclerochronological investigation of a modern biological invasion in San Francisco Bay, United States. Palaios 25 (5), 742–753.
Harzhauser, M., Piller, W.E., Müllegger, S., Grunert, P., Micheels, A., 2011. Changing seasonality patterns in Central Europe from Miocene Climate Optimum to Miocene Climate Transition deduced from the *Crassostrea* isotope archive. Global and Planetary Change 76, 77–84.
Killingley, J.S., Berger, W.H., 1979. Stable isotopes in a mollusc shell: detection of upwelling events. Science 205, 186–188.
Kirby, M.X., 2000. Paleoecological differences between Tertiary and Quaternary *Crassostrea oysters*, as revealed by stable isotope sclerochronology. Palaios 15, 132–141.
Lazareth, C.E., Vander Putten, E., André, L., Dehairs, F., 2003. High-resolution trace element profiles in shells of the mangrove bivalve *Isognomon ephippium*: a record of environmental spatio-temporal variations? Estuarine, Coastal and Shelf Science 57, 1103–1114.
Lorrain, A., Paulet, Y.M., Chauvaud, L., Dunbar, R., Mucciarone, D., Fontugne, M., 2004. $\delta^{13}C$ variation in scallop shells: increasing metabolic carbon contribution with body size? Geochimica et Cosmochimica Acta 68, 3509–3519.
Luengen, A.C., Raimondi, P.T., Flegal, A.R., 2007. Contrasting biogeochemistry of six trace metals during the rise and decay of a spring phytoplankton bloom in San Francisco Bay. Limnology and Oceanography 52, 1112–1130.
McConnaughey, T.A., Gillikin, D.P., 2008. Carbon isotopes in mollusk shell carbonates. Geo-Marine Letters 28, 287–299.
McConnaughey, T.A., Burdett, J., Whelan, J.F., Paull, C.K., 1997. Carbon isotopes in biological carbonates: respiration and photosynthesis. Geochimica et Cosmochimica Acta 61, 611–622.
Mook, W.G., Tan, F.C., 1991. Stable carbon isotopes in rivers and estuaries. In: Degens, E.T., Kempe, S., Richey, J.E. (Eds.), Biogeochemistry of Major World Rivers. John Wiley and Sons Ltd, pp. 245–264.
Mook, W.G., Vogel, J.C., 1968. Isotopic equilibrium between shells and their environment. Science 159, 874–875.
Parker, S.R., Gammons, C.H., Poulson, S.R., DeGrandpre, M.D., Weyer, C.L., Smith, M.G., Babcock, J.N., Oba, Y., 2010. Diel behavior of stable isotopes of dissolved oxygen and dissolved inorganic carbon in rivers over a range of trophic conditions, and in a mesocosm experiment. Chemical Geology 269, 22–32.
Pearce, N.J.G., Perkins, W.T., Westgate, J.A., Gorton, M.P., Jackson, S.E., Neal, C.R., Chenery, S.P., 1997. A compilation of new and published major and trace element data for NIST SRM 610 and NIST SRM 612 glass reference materials. Geostandards Newsletter 21, 115–144.
Pilkey, O.H., Goodell, H.G., 1963. Trace elements in recent mollusk shells. Limnology and Oceanography 8, 137–148.
Poulain, C., Lorrain, A., Mas, R., Gillikin, D.P., Dehairs, F., Robert, R., Paulet, Y.-M., 2010. Experimental shift of diet and DIC stable carbon isotopes: influence on shell $\delta^{13}C$ values in the Manila clam *Ruditapes philippinarum*. Chemical Geology 272, 75–82.
Richardson, C.A., 2001. Molluscs as archives of environmental change. Oceanography and Marine Biology: Annual Review 39, 103–164.
Schemel, L.E., Brown, R.L., Bell, N.W., 2003. Salinity and temperature in South San Francisco Bay, California, at Dumbarton Bridge: Results from the 1999–2002 water years and an overview of previous data. United States Geological Survey, Water Resources Investigations Report 03-4005.
Spiker, E.C., 1980. The behavior of ^{14}C and ^{13}C in estuarine water: effects of in situ CO_2 production and atmospheric exchange. Radiocarbon 22, 647–654.
Spiker, E.C., Schemel, L.E., 1979. Distribution and stable isotope composition of carbon in San Francisco Bay. In: Conomos, T.J. (Ed.), San Francisco Bay: The Urbanized Estuary. Pacific Division: American Association for the Advancement of Science, San Francisco, pp. 195–212.
Stecher, H.A., Krantz, D.E., Lord, C.J., Luther, G.W., Bock, K.W., 1996. Profiles of strontium and barium in *Mercenaria mercenaria* and *Spisula solidissima* shells. Geochimica et Cosmochimica Acta 60, 3445–3456.
Surge, D., Lohmann, K.C., Dettman, D.L., 2001. Controls on isotopic chemistry of the American oyster, *Crassostrea virginica*: implications for growth patterns. Palaeogeography, Palaeoclimatology, Palaeoecology 172, 283–296.
Tamelander, T., Kivimäe, C., Bellerby, R.G.J., Renaud, P.E., Kristiansen, S., 2009. Base-line variations in stable isotope values in an Arctic marine ecosystem: effects of carbon and nitrogen uptake by phytoplankton. Hydrobiologia 630, 63–73.
Tanaka, N., Monaghan, M.C., Rye, D.M., 1986. Contribution of metabolic carbon to mollusk and barnacle shell carbonate. Nature 320, 520–523.
Thébault, J., Chauvaud, L., L'Helguen, S., Clavier, J., Barats, A., Jacquet, S., Pécheyran, C., Amouroux, D., 2009. Barium and molybdenum records in bivalve shells: geochemical proxies for phytoplankton dynamics in coastal environments? Limnology and Oceanography 54, 1002–1014.
Thompson, J.K., Koseff, J.R., Monismith, S.G., Lucasa, L.V., 2008. Shallow water processes govern system-wide phytoplankton bloom dynamics: a field study. Journal of Marine Systems 74, 153–166.
Titschack, J., Zuschin, M., Spötl, C., Baal, C., 2010. The giant oyster *Hyotissa hyotis* from the northern Red Sea as a decadal-scale archive for seasonal environmental fluctuations in coral reef habitats. Coral Reefs 29, 1061–1075.
Urey, H.C., 1947. The thermodynamic properties of isotopic substances. Journal of the Chemical Society 562–581.
Urey, H.C., Lowenstam, H.A., Epstein, S.R., McKinney, C.R., 1951. Measurements of paleotemperatures and temperatures of the Upper Cretaceous of England, Denmark and the Southeastern United States. Geological Society of America Bulletin 62, 399–416.
USGS, 2011. United States Geological Survey Preliminary Certificate of Analysis. Micro-analytical Carbonate Standard, MACS-3.
Vander Putten, E., Dehairs, F., Keppens, E., Baeyens, W., 2000. High resolution distribution of trace elements in the calcite shell layer of modern *Mytilus edulis*: environmental and biological controls. Geochimica et Cosmochimica Acta 64, 997–1011.
Vinogradov, A.P., 1953. The Elemental Chemistry of Marine Organisms. Yale Peabody Museum, New Haven Connecticut. 647 pp.
Wisshak, M., López Correa, M., Gofas, S., Salas, C., Taviani, M., Jakobsen, J., Freiwald, A., 2009. Shell architecture, element composition, and stable isotope signature of the giant deep-sea oyster *Neopycnodonte zibrowii* sp. n. from the NE Atlantic. Deep-Sea Research I 56, 374–407.